Ind. J. Pharm. Edu. Res., 2025; 59(3):901-912.
https://www.ijper.org

Original Article

Development of Genistein-Loaded Nanogel for Skin Aging: An *in vitro* and *in vivo* Study

Ranjit Kumar Harwansh[1,*], Mohammad Akhlaquer Rahman[2], Rohitas Deshmukh[1]

[1]Department of Pharmaceutics, Institute of Pharmaceutical Research, GLA University, Mathura, Uttar Pradesh, INDIA.
[2]Department of Pharmaceutics and Industrial Pharmacy, College of Pharmacy, Taif University, Taif, SAUDI ARABIA.

ABSTRACT

Background: Generating Reactive Oxygen Species (ROS) at high altitudes causes several disorders, including skin aging. Genistein (GN) is a potent herbal bioactive compound found in many herbs like Soy GN has been reported to have several beneficial health effects, including antioxidant and photoprotection activities. However, their therapeutic efficacy is limited because of low solubility and poor oral bioavailability. **Objectives:** The current work was designed to formulate a nanoemulsion of GN in nanogel to ensure its enhanced bioavailability and improved UVA protection effect against oxidative stress. **Results:** The best formulation, GN-NE2, was composed of oil-labrafac Lipophile WL1349, water and S_{mix} (surfactant-labrasol and cosurfactant-PEG 400) at an optimized ratio (15:30:55% w/w), respectively. *Ex vivo* skin permeation, *in vivo* bioavailability and *in vivo* UVA protection activity of GN-NE2-based nanogel (GN-NG2) were studied using a rat skin model. GN-NG2 exhibited a sustained release profile as compared to its conventional gel. Moreover, significant skin permeability ($p<0.05$) and enhanced photo-protection potential were achieved with GN-nano gel when compared with conventional gel. **Conclusion:** GN-NG2 exhibited improved UVA protection efficacy and antioxidant effect because of enhanced trans-cutaneous absorption. Thus, nanogel could be a promising approach to combat UVA-mediated skin damage.

Keywords: Nanogel, Oxidative stress, Bioavailability, UV rays, Genistein, Nanoemulsion.

Correspondence:
Dr. Ranjit Kumar Harwansh, M. Pharm, PhD
Department of Pharmaceutics, Institute of Pharmaceutical Research, GLA University, Mathura-281406, Uttar Pradesh, INDIA.
Email: harwanshranjeet@gmail.com

Received: 16-09-2024;
Revised: 24-12-2024;
Accepted: 07-04-2025.

INTRODUCTION

High-altitude environments impose severe physiological challenges, particularly regarding the reduced oxygen level, low temperature and elevated Ultraviolet (UV) radiation.[1,2] Moreover, Reactive Oxygen Species (ROS) formation at high altitudes has been linked to various ailments, including skin disorders.[3,4] Skin is exposed to both endogenous and exogenous sources of oxidative stress and has developed multiple mechanisms to cope with increased oxidation.[5,6] Unprotected skin can burn within 6 min at 3000 m, as skin is exposed to 30% more UV than at sea level. UV [Ultraviolet radiation broadly categorized as UVA (315-400 nm) and UVB (280-315) exposure to the skin leads to various dermatological problems. The UVB radiation with wavelength ranging from (280-315 nm) predominantly affects the epidermis in which it is absorbed.[7]

In contrast, UVA radiation affects the dermis's innermost layer and alters the level of the skin's endogenous antioxidant enzymatic systems. As a result, an intermediate product ROS formed upon UV exposure to the skin.[8] This ROS may lead to oxidative stress by altering the protein and lipid function through the peroxidation. Several skin problems are produced by UV rays include wrinkle, aging, sunburn, inflammation, dermatitis, DNA damage, melanoma, etc.,[9] UV rays interact with DNA by strand breakage, nucleic acid oxidation and changes between neighboring pyrimidine bases on a single strand of DNA, resulting in the formation of thymine dimmers or Cyclopyrimidine Dimmers (CPDs). These alterations led to mutations and carcinoma of skin cells.[7,8] Cellular antioxidant consequence leads to increased level of Thiobarbituric Acid Reactive Substances (TBARS) and reduced level of Glutathione (GSH),[10] Catalase (CAT), Superoxide Dismutase (SOD) and Glutathione Peroxidase (GPX).[11] Antioxidant-based non-novel skin formulations can protect up to some extent but not for a longer duration of action against UV irradiation in high altitude regions which need to be applied frequently.[11] UVA plays a major part in skin aging, loss of collagen and development of wrinkles and contributes to the development of skin cancer. Nutraceuticals and functional foods are bioactive compounds present in food and dietary supplements at a relatively low amounts that benefit human health by preventing several diseases.[12]

DOI: 10.5530/ijper.20256890

Genistein [4', 5,7-trihydroxy isoflavone, (Figure 1)], mainly found in dietary and food plants, is one such nutraceutical that has been widely reported.[13,14] GN is the main biologically active compound of the perennial herb Glycine max (soybean), which finds its use as a dietary supplement and herbal medicine for managing human healthcare throughout the world.[15-17] GN protects the human skin against UVB-induced photoaging and photodamage.[18-20] GN has been well reported for their other potential therapeutic benefits like antioxidant, anti-inflammatory, hepatoprotective, antiobesity, antidiabetic, anti-cancer and anti-osteoporosis.[21-23] GN is a BCS-II molecule (low solubility and high permeability) suffer from poor solubility as well as low bioavailability due to its rapid absorption and clearance from the small intestine and liver, respectively. Reported log P (partition coefficient) of GN is about 2.96 which means it is lipophilic compound. Despite their several therapeutic benefits, GN is quickly eliminated from the body due to extensive hepatic first-pass metabolism leading to a short half-life of about 4 hr and 24% oral bioavailability.[24-26]

Nanocarriers could deliver the drug for a more extended period at a controlled rate. The goal of the nanocarrier is to increase the solubility and permeability of poorly aqueous molecules with the help of novel carriers like Nanoemulsions (NEs).[27-29] Nanoemulsion is a thermodynamic stable system that may be defined as a homogeneous system of oils, surfactants and co-surfactants (S_{mix}) and an aqueous phase in an appropriate ratio having droplet size in the range of 20-200 nm.[30-32] Nanoemulsion-based drug delivery systems have become a valuable means for encapsulating, protecting and delivering poorly soluble nutraceuticals as well as drugs.[33]

NEs have certain advantages due to their ease of formulation, simplified fabrication and easily scaled-up feasibility.[34-37] The poor solubility of GN offers a novel formulation for bioavailability enhancement and better therapeutic benefits.

Thus, the study aimed to enhance GN solubility by using a nanoemulsion as a nanocarrier system and to prepare GN nano-gel for transdermal application against high-altitude UVA-induced skin damage.

MATERIALS AND METHODS

Chemicals

Genistein (Sigma-Aldrich, MO) was used as a drug molecule. Gift samples such as transcutol, isostearyl isostearate, lauroglycol 90, plurol isostearique, plurol oleique, labrasol and labrafac WL1349 were received from Gattefossé, Saint-Priest, France. From ABITEC Corporation, USA, Acconon CC-6 was obtained. All the chemicals and reagents used in the study were of analytical grade. Milli-Q water was prepared from Millipore, MA, purification system.

RP-HPLC Analysis of GN

Estimation of GN in the formulation and excipients was done by the RP-HPLC method. The Waters HPLC system was used for analysis. It consists of a PDA detector, rheodyme-7725i injection valve, sample loop (20 µL), quaternary pump and vacuum degasser. Empower-2 software was used for data analysis. For the separation of a compound, the C_{18} guard column (10×3.0 mm) and Spherisorb C_{18} column (250 mm×4.6 mm, 5 µm) were used. Chromatographic conditions such as 15 min run time, temperature (25±0.5°C), wavelength (260 nm) and flow rate (1 mL/min) were maintained for analysis. Microsyringe (20 µL) was used for injecting the sample into the injection port.

The stock solution of GN (1000 µg/mL) was prepared in methanol. Different concentrations of GN samples were prepared from the stock solution and kept in the refrigerator until further use. Different ratio of methanol and water (25:75, 30:70, 65:35 v/v) was performed in isocratic mode. pH of the mobile phase was adjusted up to 2.5 using 1% glacial acetic acid. Pre-filtered samples were used in this study. All the samples were run in triplicate (n=3). GN content was estimated by comparing the peak area of the sample with pure GN. As per ICH guidelines, a method was developed and validated for GN.

Screening of GN Solubility in Excipients

Solubility study of GN was studied in different excipients, including Olive Oil (OL), Isopropyl Myristate (IPM), Sesame Oil (SO), Oleic Acid (OA), LLW, Eucalyptus Oil (ELO), Ethyl Oleate (EO), Soybean Oil (SBO), Isostearyl Isostearate (ISIS), Liquid Paraffin Oil (LPO) and Milli-Q water. For the solubility study, a 2 mL capacity Eppendorf tube was selected in which 1 mL of each oil phase and an excess amount of GN was added separately. To get equilibrium isothermal shaker was used for 72 hr at room temperature.[38] The supernatant layer was collected after centrifugation at 13500 rpm for 5 min and analyzed by RP-HPLC at 260 nm.

Selection of Surfactants and Co-surfactants

For the formulation of NEs, various kinds of surfactants and cosurfactants were selected. For example, Brij 35, tween 80, span 80, lauroglycol 90, acconon CC-6 and labrasol was used as a surfactant, while plurol oleaque, plurol isostearate, PEG 400 and transcutol-CG was used as a cosurfactant. For testing, 2.5 mL of 15% w/w of surfactant solution was prepared, which was utilized further for dissolving the oil phase with the help of a vortex mixer.

Construction of Phase Diagram

LLW, labrasol, PEG 400 and purified water were chosen to develop phase diagrams. Different S_{mix} ratio of 1:0 to 1:3% was optimized for the preparation of NEs. The aqueous titration method was used to construct a phase diagram in between oil, S_{mix} and water. Briefly, water was added dropwise into the mixture of oil and S_{mix}

to prepare NEs. According to the flow and transparent features of the system, different NEs regions were designed. Various Oil:S_{mix} ratios of 1:9 to 9:1% w/w were made to get suitable formulations. Phase diagrams were denoted by triangle apex, oil, water and S_{mix}, respectively. Further, it was designed to evaluate the formulations for their physical stability.[39]

Evaluation of Formulations for Thermodynamic Stability

To ensure the physical stability of NEs, thermodynamic tests, including freeze-thaw, heating-cooling and centrifugation, were conducted.[39] Different formulations were chosen from a nanoemulsion region of each phase diagram so the maximum amount of the drug could be dissolved into the oil phase. Different NE_S (o/w) were prepared by spontaneous nanoemulsification and ultrasonication process in which a concentration of GN was added up to 1 mg/mL.

Assessment of Conductivity, %Transmittance, Viscosity, pH and Refractive index

Different GN-loaded NEs were evaluated for conductivity, % transmittance, viscosity, pH and refractive index according to the procedure reported by Harwansh *et al*., (2015).

Drug Loading and Entrapment Efficiency

Estimating drug loading and entrapment efficiency in the formulations was done by procedure reported by Harwansh *et al*., (2015). In brief, pure drugs were separated from formulations by ultra-filtration and centrifugation techniques. Millipore ultra-filtration unit (10000 Da) and SpinWin MC02 (13500×g) were used for the separation of the drug from the formulation. The supernatant layer was taken and appropriately diluted with methanol prior to analysis. The drug content in the formulation was quantified by the HPLC method at 260 nm.

Droplet Size and Zeta Potential Measurement

For measurement of zeta potential and droplet size of the NEs, Zetasizer, NanoZS90 Malvern Instruments Ltd, UK was used. Measurement was done at 50 mV lasers at a fixed angle of 90° for 2 min and 12 sub-runs at room temperature (25±0.5°C).

Transmission Electron Microscopy (TEM)

For surface and morphology behavior Jeol, Jem 2100, USA, the transmission electron microscope was used. In brief, the formulation was applied on a 300-mesh size carbon-coated grid with a working voltage of 200 kV. The sample was stained by using phosphotungstic acid and dried at room temperature. Then smear was scanned at various magnifications to take images.

UV-spectrum Analysis

Multiskan-Go Thermo scientific USA UV-visible spectrophotometer was used for spectrum analysis of pure GN, placebo and formulation, GN-NE2. Quartz microplate 96-well was used for simultaneous estimation of a sample.

HPTLC Analysis

For HPTLC chromatographic fingerprint, the CAMAG Switzerland instrument was used along with the Linomat V sample applicator and Wincats software. In brief, for elution of the compound mobile system of toluene: ethyl acetate: formic acid (7:3:0.5 v/v/v) was optimized. The sample was applied on the pre-coated aluminium TLC plate and UV densitometry scanning was made at 260 nm.

IR-spectrum Analysis

FTIR Perkin Elmer USA machine was used for the spectroscopic study of pure GN and formulation for their compatibility with each other. Spectrum was recorded from 4000-500 cm^{-1}.

Accelerated Stability Test

According to the ICH guideline accelerated stability test was conducted at 40±2°C/75±5% RH. Prior to analysis, a sample was kept in airtight container and placed in a stability chamber for some time. Initially, it was stored for 0 and 90 days. The sample was checked at regular intervals of 30, 60 and 90 days for any physical and chemical changes in the formulation. The drug content in the formulation was estimated by the HPLC method.

Development of Genistein-Loaded Gel Formulations

GN-loaded different gel formulations were developed according to our previously reported method by Harwansh *et al*.[35] A conventional gel of Genistein (GN-CG≈0.1 g of GN) was designed with carbopol 940 gel base and other excipients. Carbopol 940-based gel (10 mg/mL) was prepared using distilled water in which 10 g of each excipient, such as isopropyl alcohol, PG and PEG 400 were incorporated. This dispersion system was kept in the dark for 24 hr to swell properly. Then, 0.5 g of Triethanolamine (TEA) was added to obtain a homogeneous mass of conventional gel. The Nanoemulsion (GN-NE2) based nano-gel (GN-NG2, ≈0.1 g of GN) and the placebo-NG2 formulation were made for further study.

Rheology and Spreadability Study

Anton Paar Rheometer, Austria, was used to measure the rheology of the formulation. Both placebo and drug-loaded formulations were analyzed for their rheological behavior. The rheological rate was performed at 0.001-100 s^{-1} and 0.0001-100 s^{-1}. Prior to stress analysis on the plate, a sample was kept for 10 min resting period.

The spreading ability of the product was performed according to the Khurana *et al*., method.[40]

Animal Study

Animals (male Wistar rats, 180-220 g) were used for an experiment. In prior studies, all the animals were acclimatized in a favorable environment of 12 hr light and dark cycles with 25°C/RH 45-55 RH. Rats were divided into 6 groups and kept in separate cages. All the animals have free access to food (pellet chow) and water ad libitum. This experiment was performed as per the approval (No. AEC/PHARM/1501/05/2015) and guideline of IEAC, CPCSEA, India.

Ex vivo Skin Permeation Study

Franz diffusion assembly was used for the skin permeability study in which excised abdominal rat skin was mounted, having a 1.77 cm^2 surface area. The receptor compartment faced the dermal side of the skin, having PBS, pH 7.4, while the donar compartment faced the stratum corneum side of the skin. The sink condition was maintained at a temperature of 37±0.5°C and diffusion fluid was stirred by using a magnetic stirrer.

500 mg GN-NE1-4, GN-NG2 and GN-CG (≈20 mg GN) formulations were applied uniformly over the stratum corneum layer of skin exposed to the donor compartment. After application, this part was sealed with paraffin film to provide occlusive environments. 200 L of the sample was taken from the receptor compartment and the study was performed at definite periods for 24 hr. In the receptor compartment, the same volume of freshly prepared PBS-pH 7.4 was refilled to maintain equilibrium condition. Before studying, all the samples were diluted with PBS-pH 7.4. The samples were analyzed quantitatively (n=3) through RP-HPLC at 260 nm.

Evaluation of Skin Irritation

Evaluation of skin irritation of formulations like GN-NG2, GN-CG and placebo-NG4 (500 mg) have been carried out on the rat skin (n=6). Rats were monitored for 7 days for any unwanted effects (erythema and edema) that occurred on the skin or not.

Investigation of Formulations for Their Efficacy Against Oxidative Stress Induced by UVA Rays

The photoprotection efficacy of GN-loaded various gel formulations against UVA exposure was investigated according to the method described by Harwansh *et al.*[8] The animals were divided into 5 groups (n=6) to carry out the GN-based gel formulations' photoprotective efficacy. On the dorsal side of the skin, formulations were applied at the dose of 500 mg (≈20 mg GN). Animals were divided into 5 groups for the study; group I and group II were considered as non-UVA irradiated and UVA irradiated, respectively. Group III (GN-CG), group IV (GN-NG2) and group V (placebo-NG2) were studied. Except for group I, all animal groups were irradiated with UVA rays for 7 days after the immediate formulations use.

On the 8th day, all the rats were anesthetized using a diethyl ether and sacrificed. The UVA-exposed area of skin tissues (outer cutaneous: the middle epidermis and inner dermis) was dissected surgically. The excised skin was stored in a saline solution under refrigeration till further use. Skin and 0.1 M PBS (pH 7.4) were homogenized to get the suspension and then centrifuged at 13500 rpm for 5 min to obtain a clear supernatant layer. This layer was stored at -20°C till use.

Quantification of Skin Endogenous Antioxidant Enzyme Levels

The cutaneous antioxidant level of Thiobarbituric Acid Reactive Substances (TBARS) level,[41] Glutathione Peroxidase (GPX),[42] Superoxide Dismutase (SOD) level,[43] Catalase (CAT) level[44] and total protein[45] were estimated according to standard reported procedures. A multimode microplate reader (SpectraMax® M5, USA) was used for quantification of various enzyme levels.

In vivo Bioavailability Study of Pure Genistein and Nano-gel

After transdermal and oral administration of nanogel and pure GN, bioavailability was determined at the dose of GN-NG2 ≈20 mg GN. Before starting the experiment, all the experiments were acclimatized to working environmental conditions and kept fast for 10 hr. Rats were divided into 2 groups: group I was treated as a oral suspension (20 mg GN) and group II was considered

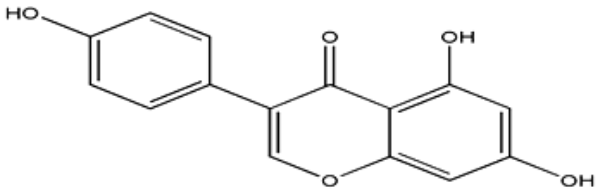

Figure 1: Genistein.

Table 1: Compositions of GN encapsulated nanoemulsion formulations.

Formulations	S_{mix} (S:Cos)	Components (%, w/w)				Oil:S_{mix}
		Oil	Water	S	Cos	
GN-NE1	1:1	10	25	32.5	32.5	1:6.5
GN-NE2	1:2	15	30	18.34	36.66	1:3.6
GN-NE3	2:1	20	36	29.34	14.66	1:2.2
GN-NE4	3:1	15	33	39	13	1:3.4

Where 'S'=Surfactant and 'Cos'= Co-surfactant.

Table 2: Genistein-loaded formulations and their physicochemical characterizations.

Formulations	Droplet size (nm)	Zeta potential (mV)	Refractive index	Conductivity (ms/cm)	pH	Viscosity (cP)	%Entrapment efficiency	%Drug loading	Polydispersity index	%Transmittance
GN-NE1	220.8±1.45	-53.2 ±0.31	1.313±0.21	0.78±0.11	6.88±0.23	10.32±0.12	88.95±0.45	0.89±0.01	0.305 ±0.06	82.86±0.23
GN-NE2	110.2±1.13	-33.1 ±0.05	1.306±0.12	0.52±0.76	7.04±0.12	9.85±0.78	99.92±0.10	1.01±0.03	0.218 ±0.03	98.95±0.83
GN-NE3	232.4±1.09	-45.5 ±0.21	1.321±0.68	0.67±0.58	7.15±0.24	12.39±0.27	90.67±0.21	0.91±0.04	0.364 ±0.01	89.26±0.19
GN-NE4	216.8±1.15	-39.3 ±0.08	1.356±0.84	0.72±0.19	6.90±0.18	14.19±0.51	92.77±0.34	0.93±0.08	0.295 ±0.07	86.78±0.95

Studies were performed in triplicate (n=3) and. Data were represented as Mean±SD.

a transdermal route (GN-NG2 ≈20 mg GN). Latin crossover[2] design was adopted for performing this experiment. Gel was administered to the skin (1.766 cm^2) with a protective layer of paraffin. From retro-orbital, a blood sample (2.5 mL) was collected at a specified time of up to 12 hr for orally and 24 hr for transdermally administered GN. Prior analysis, plasma was separated from blood and drug content was estimated by the RP-HPLC method.

Assessment of Pharmacokinetics

The pharmacokinetics of GN was assessed after the administration of pure GN suspension and GN-NG2 to each group. Phoenix WinNonlin® (version 6.4, Certara, USA) software was utilized for data integration. For the pharmacokinetic study, a non-compartment model was applied. A plot between plasma concentration and time was made and C_{max} and T_{max} were determined. Parameters such as Vd, Cl, Kel, $t_{1/2}$el, AUC_{0-t} and $AUC_{0-t\infty}$ were recorded. The peak and area (AUC_{0-t}) of gel and GN were compared and based on it; bioavailability (%F) was calculated.

Statistical Test

Graph Pad Prism software was used for statistical analysis. One-way ANOVA, Dunnet multiple comparison tests were made for data integration. Data were represented as Mean, SD and Mean±SEM (animal studies). Data were significant at *p*-value of 0.05.

RESULTS AND DISCUSSION

Validation of GN by RP-HPLC Method

Method validation of GN was done by the RP-HPLC method. Sample analysis was performed on isocratic mode with 70:30% v/v (methanol and water with pH 2.5, 1% glacial acetic) mobile system. The sample was eluted at a 1 mL/min flow rate at a controlled temperature of 25±0.5°C. GN had 6.54±0.02 min Retention time (Rt). A linear graph was obtained between peak areas versus concentration with 0.9998±0.01 correlation coefficient (r^2). Intra and inter-day precision assays were carried out at the 250-1000 ng/mL concentration levels. RSD was found to be <0.001% for both assays. LOQ (0.0242 ng/mL) and LOD (0.0080 ng/mL) were calculated. GN recovery was found to be 300.21±34.80 (100.07%), 600.98±24.51 (100.16%) and 900.06±20.52 ng/ml (100.00%) after spiking with 300 ng/mL, 600 ng/mL and 900 ng/mL respectively.

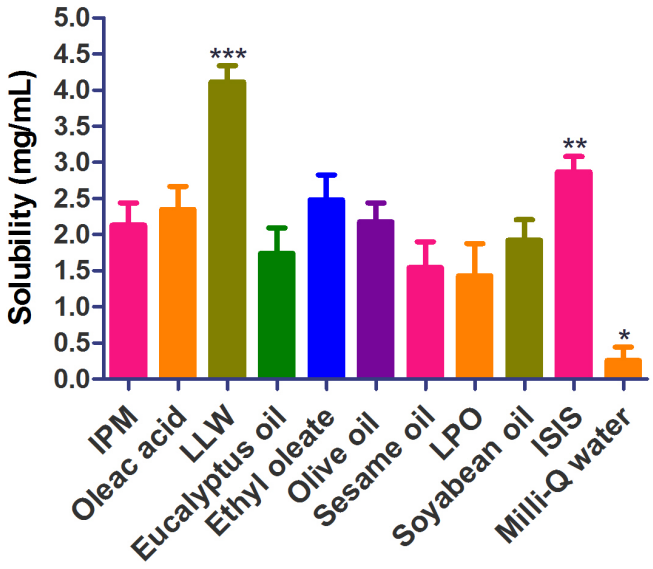

Figure 2: GN solubility profile in various oils. [*p*-value: **p* and ***p*<0.05, ****p*<0.001, Mean±SEM, (*n*=6)].

GN Solubility Profile

GN solubility in different oils was studied and their profile has been represented in Figure 2. GN was found to be at a higher maximum concentration in LLW (4.11±0.22 mg/mL) compared to others. Hence, the oil phase (LLW) was chosen for NEs preparation.

Phase Diagram

A phase diagram was constructed in between oil, water and S_{mix} to get NEs. LLW, labrasol, PEG 400 and aqueous system were optimized for further development of NEs. The pseudo-ternary phase diagram helps to get the suitable ratio of NEs components. Based on the different ratios (1:0-4:1) of S_{mix}, various plots were made, represented in Figure 3(a-g). In the case of S_{mix} (1:0), the area of nanoemulsions (o/w) was found narrow, but it was flowable, broader and stable in S_{mix} (1:1), which may be due to co-surfactant. In this ratio, intake of oil phase was found to be up to 30% in combination with 35% S_{mix}. Comparative evaluation of both S_{mix} (1:0) and S_{mix} (1:1) phase diagrams were made, which has

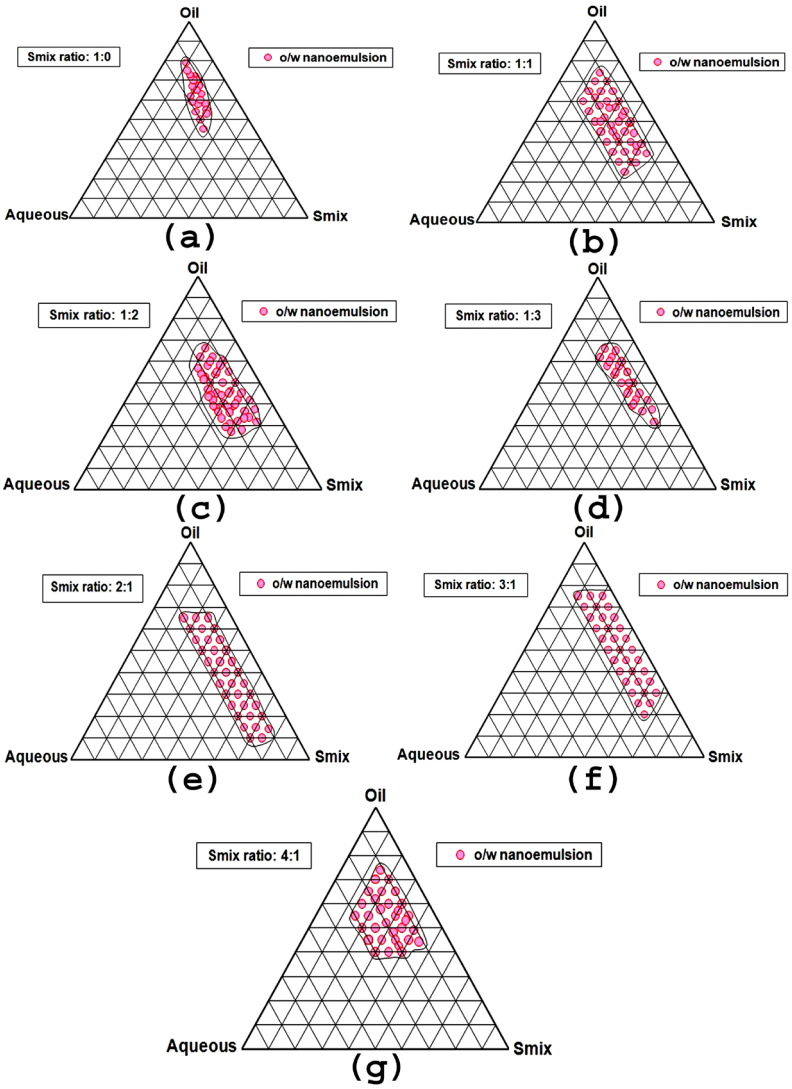

Figure 3: GN-based various phase diagrams at different S_{mix}.

been shown in the form of Figure 3a and Figure 3b respectively. In S_{mix} (1:2), the area (Figure 3c) of nanoemulsion (o/w) was good as compared with others. When the cosurfactant concentration was increased to triple at the S_{mix} ratio (1:3), the o/w NE area was not found suitable due to too preliminary NE region as compared with S_{mix} ratio (1:2) (Figure 3d). In S_{mix} (2:1) and S_{mix} (3:1), a wide and appropriate part of nanoemulsion was found, which has been represented in (Figure 3e, 3f). But an area of nanoemulsion was constricted (Figure 3g) as compared to the 1:1 ratio of $S_{mix,}$ which may be due to the high concentration of surfactant [S_{mix} (4:1)]. Comparative studies among the entire S_{mix} ratio and their phase diagrams were made. The suitable ratio was optimized as S_{mix} (1:1) for further formulation of NEs.

Test for Thermodynamic Stability

Various tests such as freeze-thaw, centrifugation and heating-cooling were applied for NEs thermodynamic stability. During the study periods, no critical events were observed; data has been provided in Supplementary Table 1.

Phase Diagram Study and Development of GN-loaded Nanoemulsions

Based on each phase diagram, a low volume of oil phase was chosen with varying amounts ranging from 10 to 30% (w/w) along with various S_{mix}. Thus, the maximum NEs region could be selected from the phase diagram. Upon incorporation of GN (1 mg/mL), no unwanted effects were seen during the formulation process. GN-based nanoemulsion compositions are mentioned in Table 1. For getting thermodynamically stable nanoemulsion formulation (o/w), labrasol (HLB=14) and PEG 400 (HLB=15.5) have been selected as surfactant and co-surfactant, respectively. Self-nano-emulsification was used for making NEs.

Physicochemical Characterization

Various physicochemical parameters such as pH, R.I., viscosity, %T, conductivity, zeta potential (Supplementary Figure 1), PDI and droplet size were used to characterize the NEs. Detailed results are shown in Table 2. Optimized nanoemulsion, GN-NE2 exhibits low PDI (0.218±0.03), confirming the formulation's uniform size. Suitable nano size (110.2±1.13 nm) and zeta potential (-33.1±0.05 mV) were achieved with GN-NE2. Zeta potential is essential for the stability of the formulation. Favorable zeta potential was obtained, which sustained the stability of the system.

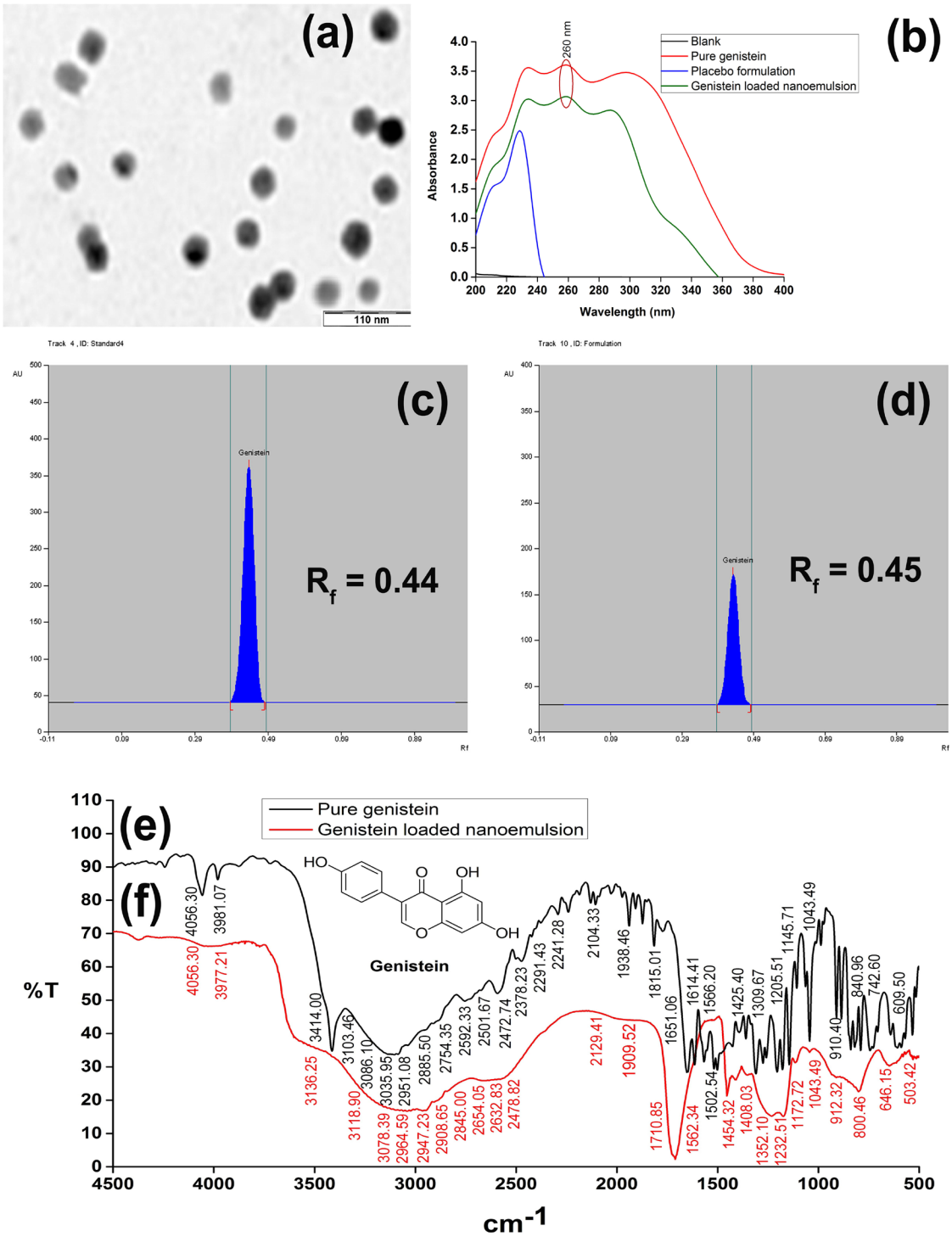

Figure 4: Image of TEM (a); UV spectrum of pure GN, placebo and GN-NE2 formulation (b); Pure GN HPTLC peak (c); and GN-NE2 (d); FTIR spectrum of pure GN (e) and GN-NE2 (f).

Microscopic and UV-spectrophotometric Study

Microscopic (TEM) analysis of GN-NE2 was made for surface behavior and the result has been shown in Figure 4 (a). Droplets were seen as dark fields which may be due to oil as a disperse phase. Results obtained from Zetasizer and TEM were closely related to each other.

From the UV spectrum study, it was confirmed that GN was present in the formulation as the spectrum showed 260 nm wavelengths similar to pure GN. The peak of GN in the formulation was little shifted. The result is represented in Figure 4(b).

HPTLC-Chromatographic Analysis

In chromatographic analysis, HPTLC chromatograms were found to be identical and sharp for pure GN (Figure 4c) and GN-NE2 (Figure 4d), having the R_f value of 0.44 and 0.45 at 254 nm, respectively as shown in Figure 4c, d. The result stated that the GN was encapsulated in the NE and no change in R_f value confirms that GN was present in the formulation and compatible with formulation ingredients.

IR-spectrum Analysis

The interaction between the drug and excipient of GN-NE2 formulation was analyzed by FTIR to check compatibility. The detailed spectrum is represented in Figure 4(e, f). GN spectrum (a) showed wave numbers at 910.40 cm^{-1} (C-H alkenes), 1043.49 cm^{-1} (-C-O alcohols), 1145.71 cm^{-1} (-OH aromatic), 1205.51 cm^{-1} (C-O alcohols), 1425.40 cm^{-1} (C-H alkanes), 1566.20 cm^{-1} (C=C aromatic ring) and 1614.41 cm^{-1} (C=C alkenes). GN phenolic hydroxyl group (O-H) stretching wave number (3414.0 cm^{-1}) was assigned. However, formulation, GN-NE2 (b) exhibited wave numbers at 910.40, 1145.71, 1205.51, 1425.40, 1566.20 and 1614.41 and 3414.00 cm^{-1} were slightly shifted to 912.32, 1172.72, 1232.51, 1502.54, 1562.34 and 3136.25 cm^{-1} respectively. Other wave numbers at 1815.01, 2104.33, 2951.08, 3035.95 and 3981.07

Table 3: Pharmacokinetic profiles of GN in rats after administration of pure GN oral suspension and GN-NG2 [Values represented were mean±SEM (*n*=6)].

Parameters	Pure GN (20 mg of GN)	GN-NG2 (~ 20 mg of GN)
C_{max} ($ngmL^{-1}$)	57.48±4.42	95.06±4.09
T_{max} (hr)	4.34±0.12	6.53±0.19
AUC_{0-t} ($nghmL^{-1}$)	251.06±8.81	885.20±63.27
$AUC_{0-t\infty}$ ($nghmL^{-1}$)	266.81±5.09	911.55±69.11
$t_{1/2}$el (h)	2.53±0.68	3.81±0.25
Kel (h^{-1})	0.27419±0.06	0.18150±0.01
Cl (Lh^{-1})	0.07967±0.01	0.02259±0.02
Vd (L)	0.29056±0.07	0.12446±0.04
%F	-	352.58

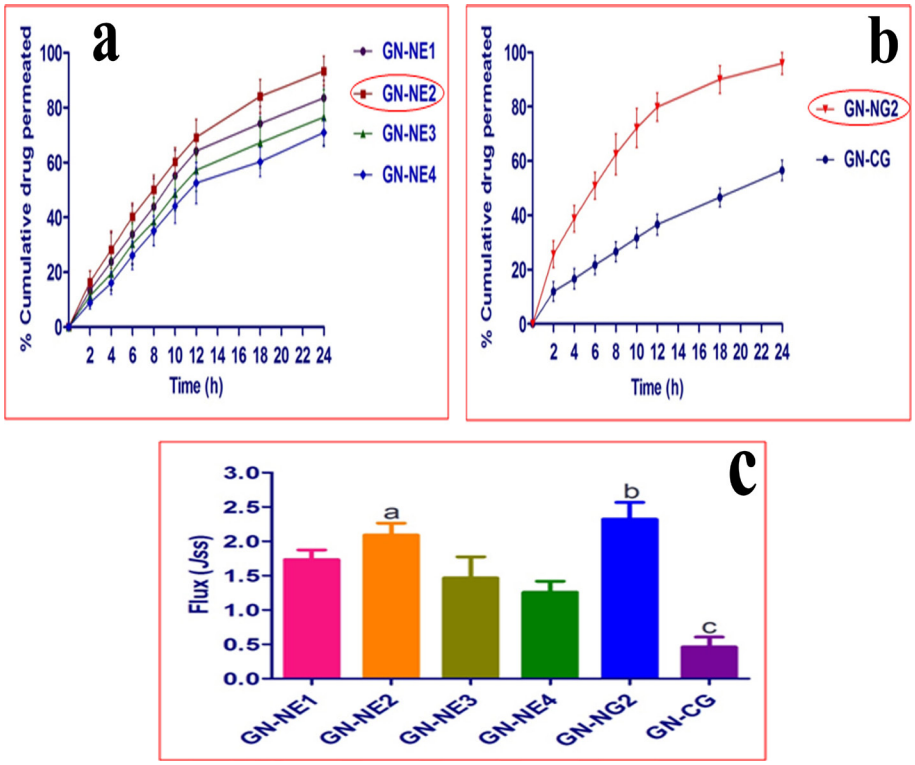

Figure 5: Permeability studies of various formulations, GN-NE1-4 (a), GN-CG and GN-NG2 (b) and Css flux (c). Data was represented as mean±SEM and the experiment was performed in triplicate. Significant *p* value was found to be $^{a,b}p<0.01$, $^{c}p<0.05$.

cm^{-1} were also slightly shifted to 1710.85, 2129.41, 2964.59, 3078.39 and 3977.21 cm^{-1} correspondingly. Minor changes in the spectrum wave number persisted, bonding of water molecules in the formulation and -OH groups in the GN structure (coordination covalent) which might be a reason for this shifting. No profound effect was observed. Finally, it can be concluded that GN was entirely compatible with the formulation components.

Stability Test

GN-NE2 was checked for stability at 40°C for more extended periods (0-90 days). GN-NE2 was evaluated based on its pH, size, electric potential (zeta) and drug content. No apparent result was seen during the study periods and detailed result has been provided in Supplementary Table 2. GN was assayed for first-order degradation kinetics at the storage of the remaining 90 days; the result was 1.22%. The detailed result was given in Supplementary Figure 2. The data showed that GN-NE2 was stable at the accelerated conditions of 40°C for a longer duration could be 2.98 years, was estimated t_{90} for it.

Viscosity

The rheological property was checked for placebo-NG2 and GN-NG2. The value 1910-3.14 Pa.s and 20-0.0268 Pa.s were observed for GN-NG2 and placebo, respectively. The inclusion of GN into the carbopol gel matrix results in a closed structure and could be the reason for the higher viscosity for GN-NG2 than the placebo. GN-NG2 exhibited shear thinning properties because of its non-Newtonian behavior. Upon high shear stress rate, viscosity decreases. This behavior is most suitable for TDDS. The result was provided as Supplementary Figure 3.[8]

Spreadability

The semi-solid gel formulations (placebo-NG2 and GN-NG2) exhibited good spreadability at 60.67±0.21 and 62.98±0.15% w/w, respectively, confirming their transdermal application use. No remarkable changes were seen for the formulation and a significant result ($p<0.05$) was obtained.

Permeability Profiles

GN permeability was evaluated using formulations such as GN-NE1-4, GN-NG2 and GN-CG. Results were represented graphically in Figure 5(a, b). Optimum skin permeability (93.81±3.33%) was achieved with the GN-NE2 compared to other formulations for 24 hr. Skin permeability of GN-NG2 and GN-CG was found to be 95.99±2.70 and 56.57±1.86% for 24 hr, correspondingly. GN-NG2 showed the best result among others.

The transdermal steady state, Jss (μg/h/cm^2) flux and Kp (cm/h) permeability coefficient [denoted by] for different formulations were represented graphically in Figure 5(c). Permeability (0.0994±0.03 cm/h) and optimum steady flux (2.322±0.42 μg/h/cm^2) were found to be statistically significant for GN-NG2 ($^{a,b}p<0.01$) among others. 0. 0.27 hr was the lag time for GN-NG2.

Nano-gel showed enhanced drug skin permeability through the transdermal route, which may result from drug content being released in a controlled manner. Labrasol and PEG 400 also acted as drug permeation enhancers by interacting with the stratum corneum. Skin permeation data of GN-CG and GN-NG2 were fitted with different kinetic models such as Zero-order model, First-order model, etc. The coefficient (r^2) was found to be 0.992 and 0.937 for GN-NG2 and GN-CG, respectively, which exhibited the Korsmeyer-Peppas pattern. Notably, GN-NG2 showed release behavior by erosion of the matrix and diffusion. In case if 0.5<Kp<1 is there, a non-Fickian pattern of the drug release model was followed.

Skin Sensitivity Test

Optimized formulation was evaluated for skin sensitivity and no harmful effect (edema, erythema and irritation) had persisted during the study. It indicates the non-irritant and safe nature of GN-based nano-gel formulation.

UV Protection Efficacy of Formulations

The efficacy of GN-based formulations was studied against UV-induced oxidative stress. The detailed result has been represented in Figure 6 (a, b). The skin antioxidant enzymes level [Figure 6(a, b)] of was decreased significantly in group II compared to control group I. The levels of enzymatic systems like CAT, GPX and SOD have been significantly improved in test groups (III and IV) upon application of GN-CG ($^{c}p<0.05$) and GN-NG2 ($^{a,b}p<0.01$), respectively, as compared with group II. Group V did not produce a significant antioxidant effect as compared to group II, as is expected from a placebo gel (without GN). Decreased TBRAS level was achieved significantly with nano-gel compared to the group irradiated with UVA ($^{a,b}p<0.01$). Gel without nanocarrier exhibited minimal therapeutic efficacy while nano-gel showed remarkable results, possibly due to the better penetrability of the formulation to the deepest skin layers and reach to blood circulation.[46] In addition, nano-gel exhibited therapeutic effects in a sustained manner which is good for treating and preventing UV-induced oxidative stress. A current study demonstrated that the delivery of genistein through a topical route in the form of nano-gel can avoid hepatic first-pass metabolism and result in the prolongation of drug action. Thus, the genistein-loaded nano-gel could be promising for the management of photoaging.[47-50]

Pharmacokinetic Profile

The pharmacokinetic profile of Genistein and Nanogel (GN-NG2) was studied at the dose of 20 mg. detail has been depicted in Table 3 and Figure 6c. Pure GN showed results quickly, while nano-gel exhibited better skin permeability for 24 hr. Different parameters

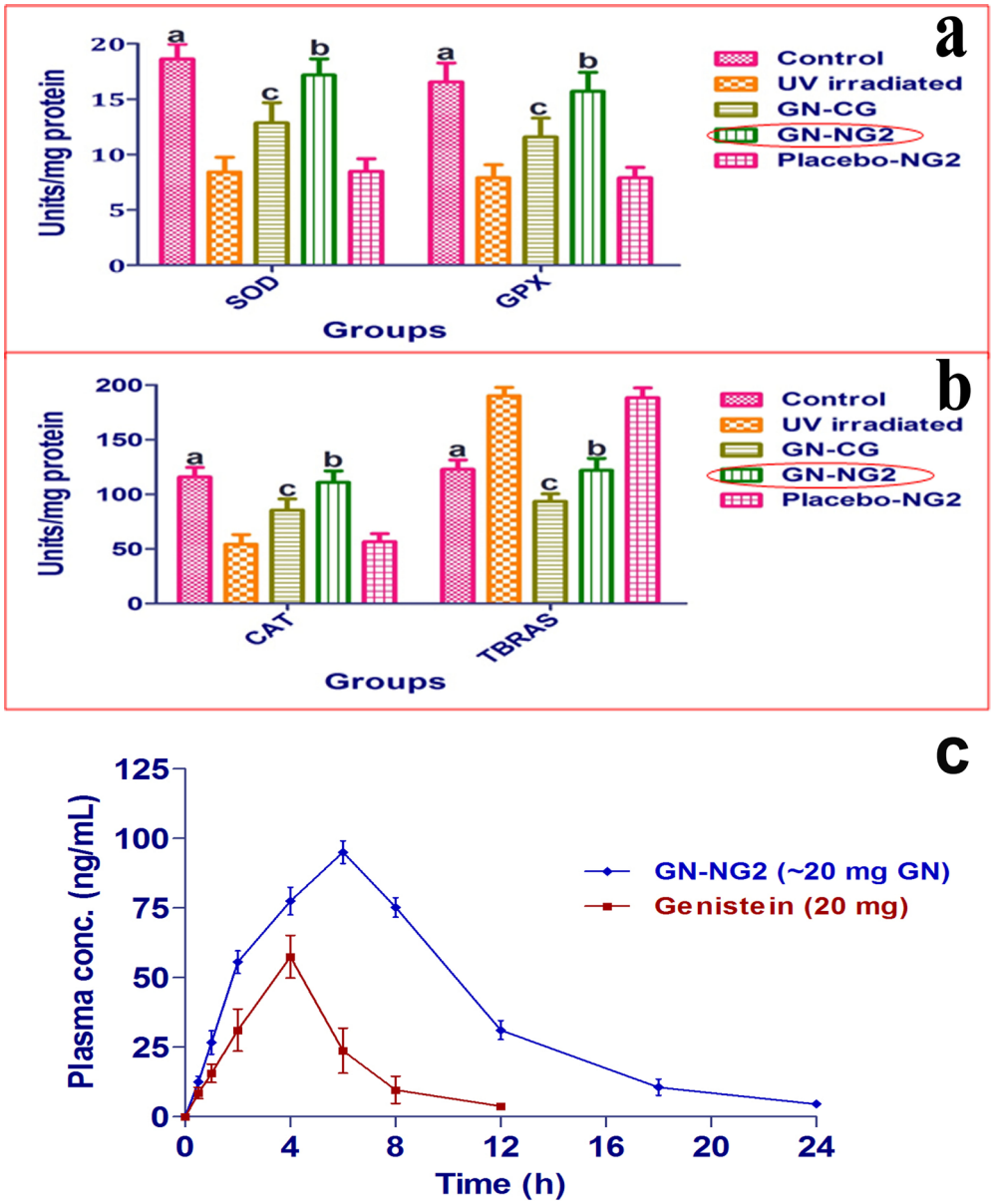

Figure 6: Endogenous skin antioxidant profile of GN-based various formulations, (a) Glutathione Peroxidase (GPX) and Superoxide Dismutase (SOD), (b) Thiobarbituric Acid Reactive Substance (TBARS) and Catalase (CAT) and pharmacokinetic profiles of genistein and GN-NG2. Mean±SEM represented values. An experiment was performed by using 6 animals in each group (n=6). *P value* ($^{a,b}p$<0.01, ^{c}p<0.05) represented the significance of the results.

such as AUC, T_{max} and C_{max} were calculated for GN and nanogel. They were found to be significant statistically (p<0.05). Maximum concentration (C_{max}) of GN from nanogel (95.06±4.09 $ngmL^{-1}$) and oral suspension (57.48±4.42 $ngmL^{-1}$) was obtained. T_{max} and $AUC_{0-t\infty}$ were higher, 6.53±0.19 hr and 911.55±69.11 $nghrmL^{-1}$ with nanogel when compared to pure GN. In case of GN-NG2, Cl, Kel and half-life ($t_{1/2}$el) was found to be 0.02259±0.02 Lhr^{-1}, 0.18150±0.01 hr^{-1} and 3.81±0.25 hr respectively. The relative bioavailability was estimated to be 3.52. It indicates that improved bioavailability of GN was achieved due to the bypass of presystemic metabolism. Moreover, transdermally, enhanced pharmacokinetic profile of GN was obtained.

Reported oral bioavailability of GN (20 mg/kg) was ~24% because of its extreme presystemic biotransformation processes.[24] The present study stated that Fr was found to be increased by 3.52 times by transdermal route. It indicates enhanced bioavailability of genistein when administered as nano-gel through the transdermal route and avoidance of the first-pass effect. It was obtained because of nanogel, which exhibits activity for prolonged period.

CONCLUSION

In summary, intense UV radiation interacts with the cutaneous antioxidant system and intervenes in oxidative stress. ROS is generated as an intermediate product upon UVB irradiation at high altitude to the skin, which results in structural and functional alteration by damaging mitochondria, DNA, proteins, lipids and endogenous enzymatic systems. These deformations lead to melanoma, skin aging and wrinkle. To combat these issues, herbal antioxidants like genistein are pioneering. Genistein-loaded nanogel can rejuvenate at altered antioxidant levels of CAT, SOD, GPX and TBRAS. Transdermally applied nanogel could enhance the UV protection efficacy and bioavailability of GN. The therapeutic effect was maintained against UVA rays for prolonged times. The developed novel nanogel (GN-NG2) was considered safe for topical uses against sunlight. Thus, genistein-loaded nano-gel could be promising for managing skin aging against extreme sun light-mediated high altitude-induced oxidative stress.

ACKNOWLEDGEMENT

The authors extend their appreciation to Taif University, Saudi Arabia for supporting this work through project number (TU-DSPP-2024-156). Authors are also thankful to the IPR, GLA University, Mathura for providing necessary facilities to accomplish the work.

FUNDING

This research was funded by Taif University, Saudi Arabia, Project No. (TU-DSPP-2024-156).

CONFLICT OF INTEREST

The authors declare that there is no conflict of interest.

ABBREVIATIONS

ROS: Reactive Oxygen Species; **GN:** Genistein; **UV:** Ultraviolet; **GN-NE2:** Genistein Loaded Nanoemulsion; **GN-NG2:** GN-NE2 Based Nanogel; **CPDs:** Cyclopyrimidine Dimmers; **CAT:** Catalase; **FTIR:** Fourier Transforms Infrared; **GPX:** Glutathione Peroxidase; **ICH:** International Conference on Harmonization; **TEM:** Transmission Electron Microscopy; **SGF:** Simulated Gastric Fluid; **SOD:** Superoxide Dismutase; **TBRAS:** Thiobarbituric Acid Reactive Substances; **NEs:** Nanoemulsions; **PBS:** Phosphate Buffer Saline; **PDI:** Poly Dispersity Index.

REFERENCES

1. Blumthaler M, Ambach W, Ellinger R. Increase in solar UV radiation with altitude. J Photochem Photobiol B. 1997;39(2):130-4. doi: 10.1016/S1011-1344(96)00018-8.
2. Bickler PE, Buck LT. Hypoxia tolerance in reptiles, amphibians and fishes: life with variable oxygen availability. Annu Rev Physiol. 2007;69:145-70. doi: 10.1146/annurev.physiol.69.031905.162529, PMID 17037980.
3. Nita M, Grzybowski A. The role of the reactive oxygen species and oxidative stress in the pathomechanism of the age-related ocular diseases and other pathologies of the anterior and posterior eye segments in adults. Oxid Med Cell Longev. 2016;2016:3164734. doi: 10.1155/2016/3164734, PMID 26881021.
4. Matsumura Y, Ananthaswamy HN. Toxic effects of ultraviolet radiation on the skin. Toxicol Appl Pharmacol. 2004;195(3):298-308. doi: 10.1016/j.taap.2003.08.019, PMID 15020192.
5. Kohen R, Gati I. Skin low molecular weight antioxidants and their role in aging and in oxidative stress. Toxicology. 2000;148(2-3):149-57. doi: 10.1016/s0300-483x(00)00206-7, PMID 10962134.
6. Shindo Y, Witt E, Packer L. Antioxidant defense mechanisms in murine epidermis and dermis and their responses to ultraviolet light. J Invest Dermatol. 1993;100(3):260-5. doi: 10.1111/1523-1747.ep12469048, PMID 8440901.
7. Harwansh RK, Deshmukh R. Recent insight into UV-induced oxidative stress and role of herbal bioactives in the management of skin aging. Curr Pharm Biotechnol. 2023. doi: 10.2174/1389201024666230427110815, PMID 37102487.
8. Harwansh RK, Mukherjee PK, Kar A, Bahadur S, Al-Dhabi NA, Duraipandiyan V. Enhancement of photoprotection potential of catechin loaded nanoemulsion gel against UVA induced oxidative stress. J Photochem Photobiol B. 2016;160:318-29. doi: 10.1016/j.jphotobiol.2016.03.026, PMID 27167597.
9. Mukherjee PK, Maity N, Nema NK, Sarkar BK. Bioactive compounds from natural resources against skin aging. Phytomedicine. 2011;19(1):64-73. doi: 10.1016/j.phymed.2011.10.003, PMID 22115797.
10. Campanini MZ, Pinho-Ribeiro FA, Ivan AL, Ferreira VS, Vilela FM, Vicentini FT, *et al.* Efficacy of topical formulations containing Pimenta Pseudocaryophyllus extract against UVB-induced oxidative stress and inflammation in hairless mice. J Photochem Photobiol B. 2013;127:153-60. doi: 10.1016/j.jphotobiol.2013.08.007, PMID 24041853.
11. Saija A, Tomaino A, Trombetta D, De Pasquale A, Uccella N, Barbuzzi T, et al. *In vitro* and *in vivo* evaluation of caffeic and ferulic acids as topical photoprotective agents. Int J Pharm. 2000;199(1):39-47. doi: 10.1016/s0378-5173(00)00358-6, PMID 10794925.
12. McClements DJ. Nanoscale nutrient delivery systems for food applications: improving bioactive dispersibility, stability and bioavailability. J Food Sci. 2015;80(7):N1602-11. doi: 10.1111/1750-3841.12919, PMID 26073042.
13. Cassidy A, Hanley B, Lamuela-Raventos RM. Isoflavones, lignans and stilbenes - Origins, metabolism and potential importance to human health. J Sci Food Agric. 2000;80(7):1044-62. doi: 10.1002/(SICI)1097-0010(20000515)80: 7<1044::AID-JSFA586>3.0.CO;2-N.
14. Irrera N, Pizzino G, D'Anna R, Vaccaro M, Arcoraci V, Squadrito F, *et al.* Dietary management of skin health: the role of genistein. Nutrients. 2017;9(6):622. doi: 10.3390/nu9060622, PMID 28629129.
15. Manach C, Scalbert A, Morand C, Rémésy C, Jiménez L. Polyphenols: food sources and bioavailability. Am J Clin Nutr. 2004;79(5):727-47. doi: 10.1093/ajcn/79.5.727, PMID 15113710.
16. Ososki AL, Kennelly EJ. Phytoestrogens: a review of the present state of research. Phytother Res. 2003;17(8):845-69. doi: 10.1002/ptr.1364, PMID 13680814.
17. Na Takuathung M, Klinjan P, Sakuludomkan W, Dukaew N, Inpan R, Kongta R, *et al.* Efficacy and safety of the genistein nutraceutical product containing vitamin E, vitamin B3 and ceramide on skin health in postmenopausal women: A randomized, double-blind, placebo-controlled clinical trial. J Clin Med. 2023;12(4):1326. doi: 10.3390/jcm12041326, PMID 36835861.
18. Wang YN, Wu W, Chen HC, Fang H. Genistein protects against UVB-induced senescence-like characteristics in human dermal fibroblast by p66Shc down-regulation. J Dermatol Sci. 2010;58(1):19-27. doi: 10.1016/j.jdermsci.2010.02.002, PMID 20211546.
19. Ahuja A, Gupta J, Gupta R. Miracles of herbal phytomedicines in treatment of skin disorders: natural healthcare perspective. Infect Disord Drug Targets. 2021;21(3):328-38. doi: 10.2174/1871526520666200622142710, PMID 32568024.
20. Tang SC, Hsiao YP, Ko JL. Genistein protects against ultraviolet B-induced wrinkling and photoinflammation in *in vitro* and *in vivo* models. Genes Nutr. 2022;17(1):4. doi: 10.1186/s12263-022-00706-x, PMID 35209841.
21. Behloul N, Wu G. Genistein: a promising therapeutic agent for obesity and diabetes treatment. Eur J Pharmacol. 2013;698(1-3):31-8. doi: 10.1016/j.ejphar.2012.11.013, PMID 23178528.
22. Li Y, Luo Y, Zhang X, Lin X, He M, Liao M. Combined taurine, epigallocatechin gallate and genistein therapy reduces HSC-T6 cell proliferation and modulates the expression of fibrogenic factors. Int J Mol Sci. 2013;14(10):20543-54. doi: 10.3390/ijms141020543, PMID 24129183.
23. Sharifi-Rad J, Quispe C, Imran M, Rauf A, Nadeem M, Gondal TA, *et al.* Genistein: an integrative overview of its mode of action, pharmacological properties and health benefits. Oxid Med Cell Longev. 2021; 2021:3268136. doi: 10.1155/2021/3268136, PMID 34336089.
24. Kwon SH, Kang MJ, Huh JS, Ha KW, Lee JR, Lee SK, *et al.* Comparison of oral bioavailability of genistein and genistin in rats. Int J Pharm. 2007;337(1-2):148-54. doi: 10.1016/j.ijpharm.2006.12.046, PMID 17280808.
25. Motlekar N, Khan MA, Youan BB. Preparation and characterization of genistein containing poly(ethylene glycol) microparticles. J Appl Polym Sci. 2006;101(3):2070-8. doi: 10.1002/app.23827.
26. Coutinho AJ, Pinheiro M, Neves AR, Pinto MM. Therapeutic potential of genistein: preclinical studies, clinical evidence and nanotechnology application. Curr Med

Chem. 2023;30(22):2480-517. doi: 10.2174/0929867329666221004124800, PMID 36200214.

27. Mukherjee PK, Harwansh RK, Bhattacharyya S. Bioavailability of herbal products: approach toward improved pharmacokinetics: approach toward improved pharmacokinetics. Educeds., Evidence-Based Validation of Herbal Medicine. 2015:218-45.
28. Choi AY, Kim CT, Park HY, Kim HO, Lee NR, Lee KE, *et al.* Pharmacokinetic characteristics of capsaicin-loaded nanoemulsions fabricated with alginate and chitosan. J Agric Food Chem. 2013;61(9):2096-102. doi: 10.1021/jf3052708, PMID 23414078.
29. Garg A, Dewangan HK. Nanoparticles as adjuvants in vaccine delivery. Crit Rev Ther Drug Carrier Syst. 2020;37(2):183-204. doi: 10.1615/CritRevTherDrugCarrierSyst.2020033273, PMID 32865905.
30. Harwansh RK, Patra KC, Pareta SK. Nanoemulsion as potential vehicles for transdermal delivery of pure phytopharmaceuticals and poorly soluble drug. Int J Drug Deliv. 2011;1:209-18.
31. Harwansh RK, Bahadur S, Deshmukh R, Rahman MA. Exciting potential of Nanoparticlized lipidic system for effective treatment of breast cancer and clinical updates: A translational prospective. Curr Pharm Des. 2020;26(11):1191-205. doi: 10.2174/1381612826666200131101156, PMID 32003686.
32. Singh S, Murti Y, Agrawal N. Application of nanoemulsion in tuberculosis treatment. In: Ramalingam K, editoreds. Handbook of research on nanoemulsion applications in agriculture, food, health and biomedical sciences. Hershey, PA: IGI Global; 2022. p. 169-93. doi: 10.4018/978-1-7998-8378-4.ch008.
33. Argenta DF, de Mattos CB, Misturini FD, Koester LS, Bassani VL, Simões CM, *et al.* Factorial design applied to the optimization of lipid composition of topical antiherpetic nanoemulsions containing isoflavone genistein. Int J Nanomedicine. 2014;9:4737-47. doi: 10.2147/IJN.S67732, PMID 25336951.
34. Harwansh RK, Patra KC, Pareta SK, Singh J, Rahman MA. Nanoemulsions as vehicles for transdermal delivery of glycyrrhizin. Braz J Pharm Sci. 2011;47(4):769-78. doi: 10.1590/S1984-82502011000400014.
35. Harwansh RK, Mukherjee PK, Bahadur S, Biswas R. Enhanced permeability of ferulic acid loaded nanoemulsion based gel through skin against UVA mediated oxidative stress. Life Sci. 2015;141:202-11. doi: 10.1016/j.lfs.2015.10.001, PMID 26437269.
36. Bahadur S, Pardhi DM, Rautio J, Rosenholm JM, Pathak K. Intranasal nanoemulsions for direct nose-to-brain delivery of actives for CNS disorders. Pharmaceutics. 2020;12(12):1230. doi: 10.3390/pharmaceutics12121230, PMID 33352959.
37. Harwansh RK, Deshmukh R, Rahman MA. Nanoemulsion: promising nanocarrier system for delivery of herbal bioactives. J Drug Deliv Sci Technol. 2019;51:224-33. doi: 10.1016/j.jddst.2019.03.006.
38. Shafiq S, Shakeel F, Talegaonkar S, Ahmad FJ, Khar RK, Ali M. Development and bioavailability assessment of ramipril nanoemulsion formulation. Eur J Pharm Biopharm. 2007;66(2):227-43. doi: 10.1016/j.ejpb.2006.10.014, PMID 17127045.
39. Choudhury H, Gorain B, Karmakar S, Biswas E, Dey G, Barik R, *et al.* Improvement of cellular uptake, *in vitro* antitumor activity and sustained release profile with increased bioavailability from a nanoemulsion platform. Int J Pharm. 2014;460(1-2):131-43. doi: 10.1016/j.ijpharm.2013.10.055, PMID 24239580.
40. Khurana S, Jain NK, Bedi PM. Nanoemulsion based gel for transdermal delivery of meloxicam: physico-chemical, mechanistic investigation. Life Sci. 2013;92(6-7):383-92. doi: 10.1016/j.lfs.2013.01.005, PMID 23353874.
41. Ohkawa H, Ohishi N, Yagi K. Assay for lipid peroxides in animal tissues by thiobarbituric acid reaction. Anal Biochem. 1979;95(2):351-8. doi: 10.1016/0003-2697(79)90738-3, PMID 36810.
42. Paglia DE, Valentine WN. Studies on the quantitative and qualitative characterization of erythrocyte glutathione peroxidase. J Lab Clin Med. 1967;70(1):158-69. PMID 6066618.
43. Kakkar P, Das B, Viswanathan PN. A modified spectrophotometric assay of superoxide dismutase. Indian J Biochem Biophys. 1984;21(2):130-2. PMID 6490072.
44. Beers RF, Jr., Sizer IW. A spectrophotometric method for measuring the breakdown of hydrogen peroxide by catalase. J Biol Chem. 1952;195(1):133-40. doi: 10.1016/S0021-9258(19)50881-X, PMID 14938361.
45. Lowry OH, Rosebrough NJ, Farr AL, Randall RJ. Protein measurement with the Folin phenol reagent. J Biol Chem. 1951;193(1):265-75. doi: 10.1016/S0021-9258(19)52451-6, PMID 14907713.
46. Jaiswal N, Akhtar J, Singh SP, Badruddeen, Ahsan F. An overview on genistein and its various formulations. Drug Res (Stuttg). 2019;69(6):305-13. doi: 10.1055/a-0797-3657, PMID 30517965.
47. Kim JH, Ko JA, Kim JT, Cha DS, Cho JH, Park HJ, *et al.* Preparation of a capsaicin-loaded nanoemulsion for improving skin penetration. J Agric Food Chem. 2014;62(3):725-32. doi: 10.1021/jf404220n, PMID 24417234.
48. Brownlow B, Nagaraj VJ, Nayel A, Joshi M, Elbayoumi T. Development and *in vitro* evaluation of vitamin E-enriched nanoemulsion vehicles loaded with genistein for chemoprevention against UVB-induced skin damage. J Pharm Sci. 2015;104(10):3510-23. doi: 10.1002/jps.24547, PMID 26108889.
49. de Vargas BA, Bidone J, Oliveira LK, Koester LS, Bassani VL, Teixeira HF. Development of topical hydrogels containing genistein-loaded nanoemulsions. J Biomed Nanotechnol. 2012;8(2):330-6. doi: 10.1166/jbn.2012.1386, PMID 22515085.
50. Back PI, Furtado LR, Nemitz MC, Balestrin LA, Fachel FN, Gomes HM, *et al.* Skin permeation and oxidative protection effect of soybean isoflavones from topical nanoemulsions-a comparative study of extracts and pure compounds. AAPS PharmSciTech. 2018;19(7):3029-39. doi: 10.1208/s12249-018-1133-x, PMID 30084071.

Cite this article: Harwansh RK, Rahman MA, Deshmukh R. Development of Genistein-Loaded Nanogel for Skin Aging: An *in vitro* and *in vivo* Study. Indian J of Pharmaceutical Education and Research. 2025;59(3):901-12.

Supplementary Table 1: **Evaluation of thermodynamic stability of different formulations (5% w/w increasing amount of oil).**

S_{mix} ratio (S:Cos)	Amount of excipients in formulations (% w/w)			Observations based on the preparation and thermodynamic stability studies		
	Oil	Milli-Q water	S_{mix}	H & C[a]	Cent.[b]	Freeze Tha.[c]
1:0	10	15	75	√		√
	15	25	60	√	√	
	20	30	50	√		√
	25	28	47	√		√
1:1	10	25	65	√	√	√
	15	35	50	√	√	√
	20	28	52	√	√	√
	25	30	45	√	√	√
	30	35	35	√	√	√
1:2	10	30	60	√	√	√
	15	30	55	√	√	√
	20	35	45	√	√	√
	25	38	37	√	√	√
	30	28	42	√	√	√
1:3	10	35	55	√	√	√
	15	40	45	√	√	√
	20	25	55	√	√	√
2:1	10	20	70	√	√	√
	15	28	47	√	√	√
	20	36	44	√	√	√
	25	40	35	√	√	√
	30	30	40	√	√	√
3:1	10	18	72	√	√	√
	15	33	52	√	√	√
	20	37	43	√	√	√
4:1	10	22	68	√	√	√
	15	20	65	√	√	√
	20	32	48	√	√	√
	25	36	39	√	√	√
	30	40	30	√	√	√

[a]Heating and cooling cycle (H & C); [b]Centrifugation (Cent.); [c]Freeze-thaw cycle (Freeze Tha.).

Supplementary Table 2: **Stability test of optimized GN-NE2 formulation.**

Time (days)	Temperature (°C)	Droplet size (nm)	Zeta potential (mV)	pH	% Drug remained	Log % drug remained
0	40±2 (75±5% RH)	110.07±1.04	-33.3±0.21	7.07±0.11	100.00	2.00
30		110.05±0.12	-32.9±0.12	6.65±1.15	99.62	1.9983
60		109.88±1.25	-32.6±0.38	6.78±1.10	99.23	1.9966
90		108.97±2.09	-32.7±1.02	6.85±1.08	98.78	1.9946

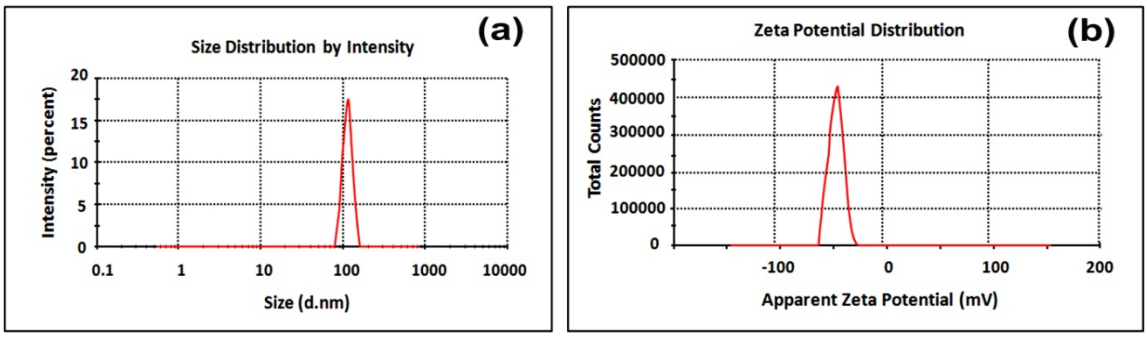

Supplementary Figure 1: Analysis of droplet size (a) and zeta potential (b) of optimized formulation, GN-NE2.

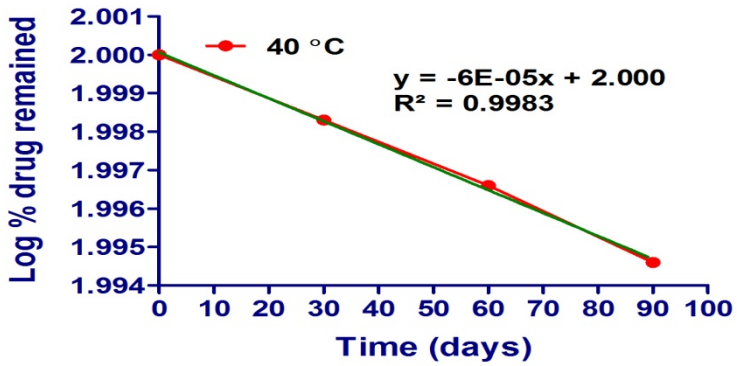

Supplementary Figure 2: Degradation kinetics of GN from GN-NE2 at 40°C.

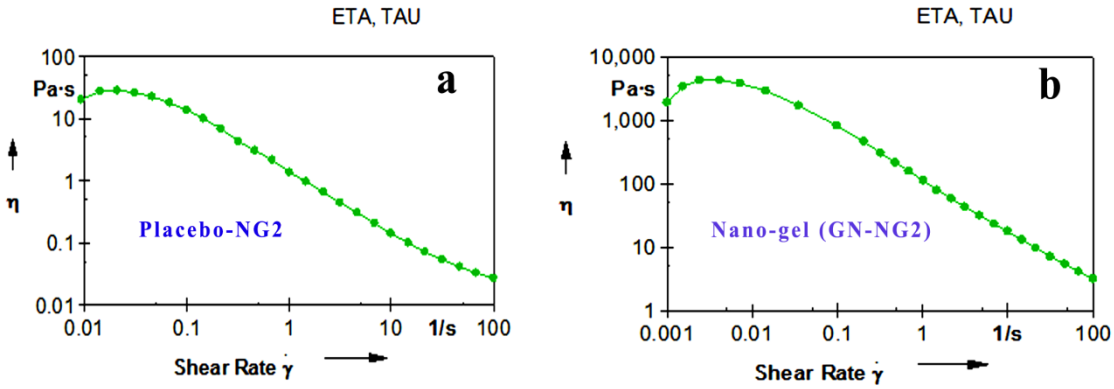

Supplementary Figure 3: Rheogram of placebo-NG2 (a) and GN-NG2 (b) where, =viscosity (Pa.s), =shear rate (1/s).